Chaos in a Spatially-Developing Plane Mixing Layer

By J. G. Broze[1], F. Hussain[1] and J. C. Buell[2]

A spatially-developing plane mixing layer has been analyzed for chaotic behavior. A direct numerical simulation of the Navier-Stokes equations in a two-dimensional domain infinite in y and having inflow-outflow boundary conditions in x was used for data. Spectra, correlation dimension and the largest Lyapunov exponent have been computed as functions of downstream distance x, over the range $0 \leq x/\delta_\omega \leq 250$, from velocity time series in an Eulerian reference frame. When forced at a single (fundamental) frequency with maximum amplitude $v'_e/\Delta U = 0.01$, the flow is periodic at the inflow but becomes aperiodic with increasing x. The aperiodic behavior is caused by the presence of a "noisy" subharmonic caused by the feedback between the necessarily nonphysical inflow and outflow boundary conditions. In order to overshadow this noise the flow was also studied with the same fundamental forcing and added random forcing of amplitude $v'_r/\Delta U = 0.01$ at the inlet. Results were qualitatively the same in both cases: for small x, spectral peaks were sharp and dimension was nearly 1, but as x increased a narrowband spectral peak grew, spectra decayed exponentially at high frequencies and dimension increased to greater than 3. Based on these results, the flow appears to exhibit deterministic chaos. However, at no location was the largest Lyapunov exponent found to be significantly greater than zero. Moderate forcing with both fundamental at $v'_e/\Delta U = 0.01$ and subharmonic at $v'_e/\Delta U = 0.01$ and 0.002 caused the flow to be periodic throughout the computational domain.

1. Introduction

The discovery of deterministic chaos in dynamical systems has opened the possibility of understanding and modelling transitional and turbulent flows, which previously could only be described statistically. Complementary to this concept, the discovery and measurement in these flows of large-scale organized vortical motions, called "coherent structures", add evidence that there is order underlying the apparent randomness of turbulence. To couple these two concepts – chaos and coherent structures – might yield working models of turbulence which do not require solution of the full Navier-Stokes equations but which may predict flow statistics and dynamics with useful accuracy. In order to do this, it must be established that chaos and coherent structures are present in flows of interest and relevant measurements must be made. It is the existence of deterministic chaos in a mixing layer which is

1 University of Houston

2 NASA Ames Research Center

the object of this study; coherent structures in mixing layers have been studied in detail previously.

Prior studies of flow chaos have been almost exclusively in closed flows, in particular, Rayleigh-Bénard convection and Taylor-Couette flow. However, most flows of interest are open flows: jets, wakes, mixing layers and boundary layers. Finding deterministic chaos in open flows is complicated by a number of factors. Most open flows, including jets, plane Poiseuille flow and spatially developing mixing layers, are convectively unstable (Bechert 1985), *i.e.*, perturbation wave packets do not remain at the point of their origin but move downstream as they grow. It might be relevant to make measurements in a reference frame moving with the disturbance; for example, Deissler & Kaneko (1987) found that solutions of the time-dependent generalized Ginzburg-Landau equation gave the appearance of being chaotic, but had no positive Lyapunov exponents until they were measured in a moving frame. However, measurements in a moving frame are quite difficult to make; laboratory techniques such as hot-wire, hot-film, or laser-Doppler anemometry are best suited to collecting time series at a single location, or in a few locations simultaneously. New techniques, such as particle displacement velocimetry, can give more spatial detail but have reduced accuracy. Numerical simulations have both spatial detail and accuracy, but an advecting probe would leave the computational domain after only about a thousand time steps, compared to tens of thousands needed for standard analysis techniques. It might also be useful to analyze instantaneous spatial data for spatial chaos. Methods for analysis of spatial data are not well established, although it is possible to apply techniques to a "space series" rather than a time series, if those data are available (Sauliere & Huerre 1988). Even so, the same obstacles to data collection apply in the spatial case as they do to the moving probe.

The flow investigated was a two-dimensional, two-stream mixing layer with $Re = (U_1 - U_2)\delta_\omega/\nu = 100$ and velocity ratio $U_2/U_1 = 0.2$. U_1 and U_2 are the velocities of the two streams, δ_ω is the inflow vorticity thickness and ν is the kinematic viscosity. All lengths and coordinates are normalized by δ_ω, and velocities by $(U_1 - U_2)$. In order to minimize the streamwise pressure gradient, entrainment velocities $v(y = -\infty) = 0.0115$ and $v(y = \infty) = -0.0044$ were imposed. The inflow profile for the streamwise velocity u was calculated from the Blasius self-similarity equation. The corresponding vertical velocity v could not be used since the self-similarity solution has vorticity at infinity. Instead, a somewhat arbitrary profile consistent with the entrainment velocities and containing a small amount of downwash was imposed at the inflow. Both velocity components were required to satisfy a "convective" outflow boundary condition of the form $\partial\phi/\partial t = -c\partial\phi/\partial x$, where $c = (U_1 + U_2)/2$. See figure 2 of Buell & Huerre (1988) for a schematic of the geometry.

Data for analysis were obtained from direct numerical simulations using a recently developed code. The two-dimensional Navier-Stokes equations are solved on a domain that is infinite in the vertical (y) direction and finite in the streamwise (x) direction. Pressure is eliminated by taking the curl of the momentum equations
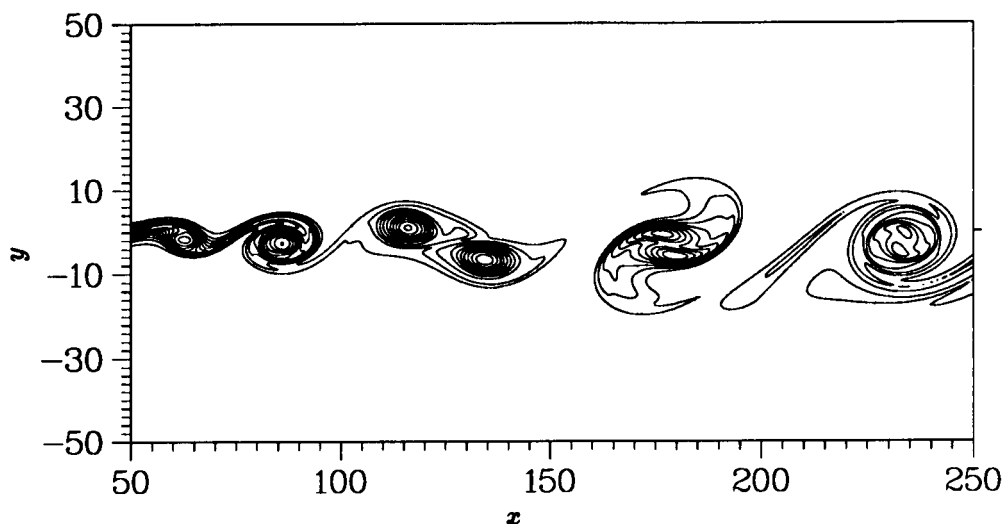
FIGURE 1. Contours of vorticity for $a = 0.01$, $b = 0.01$, $c = 0$.

twice and retaining only the x-component of the result. This yields a fourth-order equation for the streamwise velocity u which is advanced in time explicitly using a compact third-order Runge-Kutta scheme (Wray 1988). Since the Laplacian is contained in the time-derivative term, a Poisson equation must be solved during each substep. The vertical velocity v is recovered directly from the continuity equation. The numerical algorithm is based on a Fourier method with a cotangent mapping in the y direction (a modification of the method of Cain *et al.* 1984), and high-order accurate Padé approximations in the x direction. The first x-derivatives in the continuity equation and in the advection terms are approximated with modified Padé finite differencing (S. Lele, private communication). The particular approximation used here yields sixth-order accuracy for the low to moderate wavenumber components of the solution, and significantly lower dispersion errors for high wavenumbers. The second and fourth-order x-derivatives are approximated with classical fourth-order accurate Padé formulas. In order to avoid the inversion of very large sparse matrices for the solution of the Poisson equation for u, the effective wavenumber concept (Kim & Moin 1985) is applied in the x-direction so that the y-direction matrices are decoupled. The mesh used here was 384×192 in (x, y), and the domain length in the x-direction was 250. Perturbations were introduced in v at the inflow; the perturbation amplitude was tapered by a Gaussian shape over a small region near $y = 0$.

The primary instability in mixing layers is a fundamental wave which grows exponentially from its initial (linear) amplitude at the inflow, becomes nonlinear and saturates at some x, forming a rolled-up vortex. The secondary instability is the subharmonic of the fundamental which grows and saturates, resulting in vortex pairing. Both the fundamental and subharmonic are receptive to disturbances over

a band of frequencies; the initial amplitudes and phase difference control the evolution of the mixing layer. For more details, see Monkewitz (1988). The frequencies, amplitudes and phases from which these grow depend on extrinsic perturbations: controlled excitation, feedback and ambient noise. A sample vorticity plot is shown in figure 1 for a simulation with both fundamental and subharmonic perturbations. This plot shows all stages of 2-D mixing layer dynamics up through pairing. The vortex entering at $x = 60$ has not yet fully rolled up; the structure at $x = 80$ is fully formed and will eventually pair with the one at $x = 60$. Two structures near $x = 120$ are in the process of pairing, while the structures at $x = 180$ and $x = 230$ are fully paired structures.

Coflowing two stream mixing layers have been shown theoretically to be convectively unstable. However, the upstream flow can be perturbed by feedback from somewhere downstream. In experiments, this feedback may be provided by impingement on a solid body, causing pressure fluctuations which propagate upstream to the inflow, or perhaps by velocity fluctuations at the splitter plate induced by downstream vortex rollup. In numerical experiments with solid surfaces absent, this cannot occur except as boundary condition reflections. In the present numerical simulation, it was established that boundary condition reflection did exist (Buell & Huerre 1988), causing vortex rollup to occur in a nontransient manner for the conditions being simulated.

2. Approach

It is not clear whether the flow in question, a two-stream transitional mixing layer, is temporally or spatially chaotic. The flow develops in x and is obviously not spatially periodic, but it is not possible to examine the exact nature of its spatial behavior in the current framework. The flow looks somewhat more periodic in time, but closer examination reveals definite aperiodicity. It is entirely possible that the flow is both temporally and spatially chaotic. Given the inability to follow disturbances spatially for great distances, we wanted to focus more closely on temporal aspects of the flow and to exclude possible spatial dynamics. To do this, we chose to analyze time series collected in an Eulerian frame at selected flow locations and to treat streamwise distance x as a flow parameter. Since the disturbance at a given x originates upstream and convects past our "probe", we perturbed the flow by imposing a sinusoidal fluctuation (with a fundamental and/or subharmonic frequency) at the inflow boundary. This way, we imposed a periodicity on the dynamics and observed how it deviated from periodicity with increasing x. We still must rely on the presence of other disturbances to initiate this deviation, but what is of interest is how the flow organizes itself in the presence of these disturbances.

3. Excitation Case Studies

The inlet profile of the mixing layer had the form $U(y)\mathbf{i} + [V(y) + v_e(y,t)]\mathbf{j}$, where $U(y)$ is the Blasius similarity solution for a 2-D mixing layer and $v_e(y,t)$ is the perturbation. The inlet was excited with fundamental and subharmonic

perturbations and random noise with several combinations of amplitudes:

$$v_e(y,t) = f(y)\big[a\cos(\omega t) + b\cos(\omega t/2 + \phi) + c\,r(t)\big]$$

where $f(y)$ has a Gaussian shape centered at $y = 0$ and is zero elsewhere and $r(t)$ is a uniform random variable distributed on the interval (-1,1). We isolated a few key cases:

Case (i): no forcing ($a = b = c = 0$),
Case (ii): (a) fundamental only ($a = 0.01$; $b = c = 0$),
    (b) fundamental plus random forcing ($a = 0.01$; $b = 0$; $c = 0.01$),
Case (iii): fundamental and subharmonic ($a = 0.01$; $b = 0.01$, 0.002, 0.0005; $c = 0$).

In case (i), fundamental and subharmonic waves grow due to unknown perturbations arising from boundary condition reflections; low-dimensional behavior is not expected in general. In case (ii(a)), the fundamental is driven by periodic forcing, but the subharmonic is subject to background perturbation by reflections. Case (ii(b)) was used to study the difference between the subharmonic driven by background perturbation and by a random inlet forcing. In case (iii), both fundamental and subharmonic are driven by the imposed periodic perturbation. The phase angle ϕ was chosen to be 100 degrees, in the range where subharmonic enhancement is expected (Monkewitz 1988, Husain & Hussain 1988).
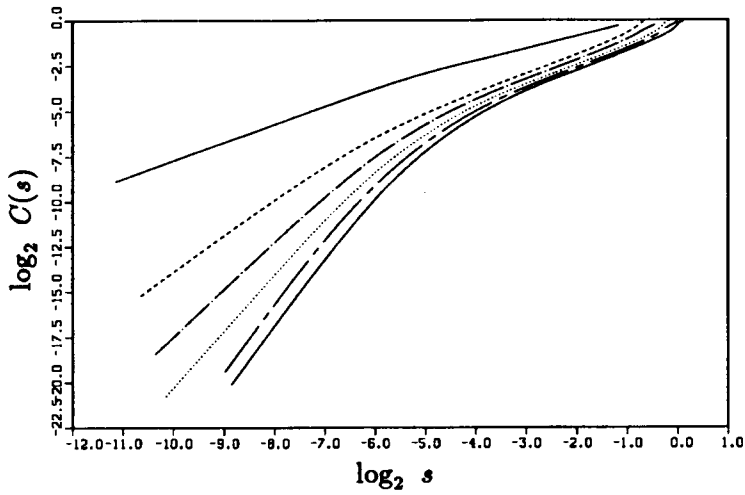
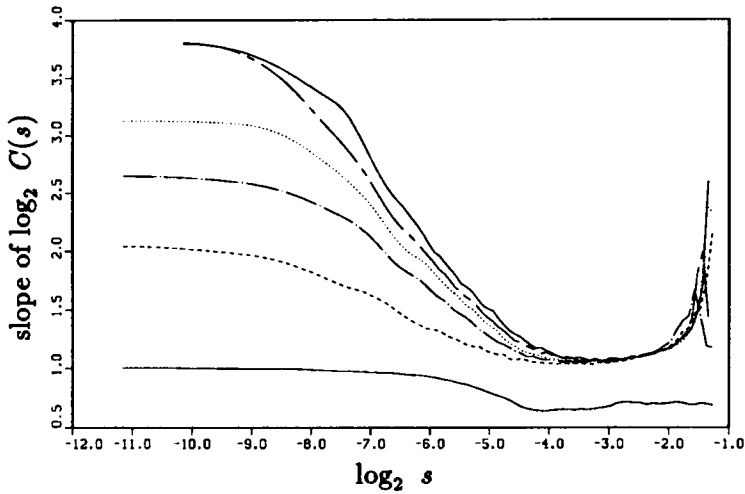## 4. Analysis Techniques

4.1. Time Series Analysis

Power spectra, correlation dimension and largest Lyapunov exponent were calculated from time series collected at selected locations in the flow domain. To establish the existence of chaos from (numerical or laboratory) experimental data is tricky, at best; several pieces of supporting evidence must be assembled and analyzed for trends as parameters are varied. Taken together, continuous spectra, noninteger correlation dimension and positive Lyapunov exponent are strong indicators of deterministic chaos.

4.1.1. Power spectra

Spectra can provide insight into flow dynamics. There are two obvious extremes: a discrete spectrum indicates periodicity or quasi-periodicity, whereas a continuous spectrum with no peaks suggests nonperiodic, random behavior. In contrast, other spectra which are intermediate cases, such as sharp peaks on broadband background noise or a combination of sharp and narrowband peaks, indicate possible low-dimensional, chaotic dynamics. The behavior of spectra at high frequencies can be used to separate deterministic chaos from randomness. In particular, the idea that exponential decay of spectra is indicative of deterministic chaos, while power-law behavior is indicative of randomness, is argued by Sigeti & Horsthemke (1987) and utilized in several studies, *e.g.*, Brandstater & Swinney (1987).

(a)

(b)

FIGURE 2.   (a) Correlation integral for case (ii(a)), $a = 0.01$, $b = c = 0$, $m = 1, \ldots, 7$ from top; (b) Slope of correlation integral, $m = 1, \ldots, 7$ from bottom.

4.1.2. Correlation dimension

The trajectories in phase space are reconstructed from a single dynamic variable using time-series-delay embedding (Takens 1980). Time delays were chosen using the first minimum of the mutual information (Fraser & Swinney 1986) and checked visually by making two-dimensional phase portraits. Correlation dimension was calculated using the algorithm of Grassberger & Procaccia (1983) (modified to use 1000 randomly chosen reference points). The correlation integral $C(s)$, where s is phase space distance, was computed for a range of embedding dimensions and fit with a cubic spline polynomial (figure 2a). Each line in the figure represents a

different embedding dimension m, increasing from top to bottom. Notice that, near the region where the $\log_2 s = -3$, all curves have approximately the same slope. The slope of C versus s was computed analytically in log-log coordinates from the spline coefficients (figure 2b). The slope is typically quite high (possibly as high as m) at the smallest distances due to the presence of noise. At larger distances, the slope drops off sharply and may flatten out; this occurs near $\log_2 s = -3$ in the example. The correlation integral is said to "scale" when the slope is constant over some range of distances and said to "saturate" when this constant slope converges as m increases. This saturated slope is called the correlation dimension ν, and is an estimate of the Hausdorff dimension. The distances over which the slope is constant is called the scaling region, since it implies that the correlation integral scales exponentially, *i.e.*, $C \sim s^\nu$. The scaling region is computed by finding the scales over which the slope does not deviate more than a given bound, typically 5%. In the example shown in figure (2b), for $m = 3$, $\nu = 1.07$ over a scaling region from $s = 0.045$ to $s = 0.20$, where s in this case is v. The actual value computed from this algorithm cannot be used to determine n very accurately; *e.g.*, it can not discriminate between 1.0 and 1.05 and therefore can not be used to "prove" that an object is fractal. It can be used to estimate dimension roughly and to measure increasing complexity as a parameter is varied. Unfortunately, data length required for the correlation dimension algorithm is large and increases roughly as k^m, where k is the some constant (Brandstater & Swinney 1987). Since higher embedding dimensions are required to reveal higher dimensional attractors, data requirements quickly get very large as dimension increases.

4.1.3. Lyapunov exponent

The largest Lyapunov exponent is a measure of the maximum rate of exponential divergence of trajectories in phase space and is indicative of chaos when positive. We calculated it using the method of Wolf *et al.* (1985). The exact value of the exponent is not crucial and should not be expected from this algorithm, although it does give results within a few percent for time series from model systems of ordinary differential equations, such as the Lorenz system. It is an important indicator of chaotic behavior, and it is important to be sure whether or not it is positive. Since the calculated exponent can vary significantly depending on input parameters (*viz.*, time delay, embedding dimension, maximum and minimum scales, evolution time), care was taken to select consistent values. The results of the correlation dimension calculation form natural choices for several of these parameters. In particular, the time delay was chosen from mutual information (the same delay was used for correlation dimension and Lyapunov exponent), embedding dimension was chosen to be the minimum m for which saturation was observed in the correlation integral, the minimum and maximum scales were taken from the limits of the flat scaling region, and the evolution time was chosen as the time delay. Several tests of these parameters were conducted. Small differences in time delay and embedding dimension had little effect on the computed exponent. However, since the algorithm follows the distance between nearby trajectories in the reconstructed phase space, minimum and maximum scales are quite important. These scale parameters sets the

range of distances between trajectories which will be considered. A distance which is too small would include the random noise at the smallest scales and might give a positive exponent even when the large-scale flow is not chaotic, while measuring at very large distances might yield a negative or zero exponent even for a chaotic attractor. The limits of the scaling region of the correlation exponent were chosen for these parameters since those are the scales over which the flow behaves as an attractor. Small variations about these values had little effect on the computed value. The choice of evolution time has some effect on the magnitude, but not on the sign, of the exponent. In summary, the exponents we calculated seem to give a good indication of the sign of the largest Lyapunov exponent.
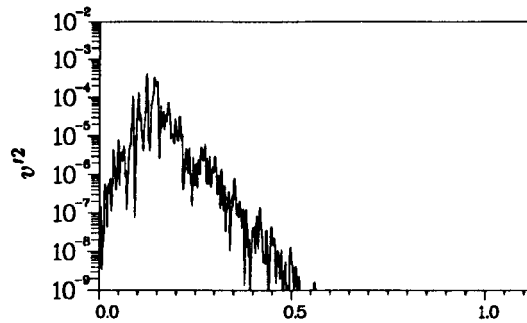
4.1.4. Flow variable

The choice of flow variable, in principle, should make very little difference in the results using these methods. Three variables were tested: u, v, and $G = \int \omega_z dy$, where ω_z is the vorticity. The v component had a smoother profile with a peak at $y \simeq 0$ while u had sharp peaks near $y \simeq 0$. The variable G was generated as a means of tracking passage of vortex peaks for use in the analysis of discrete sequences (see next section). Results were in good agreement: dimension and Lyapunov exponent using v and G were quite similar, while u tended to give slightly higher values and smaller scaling regions. After these tests, v was chosen as the variable to be used.

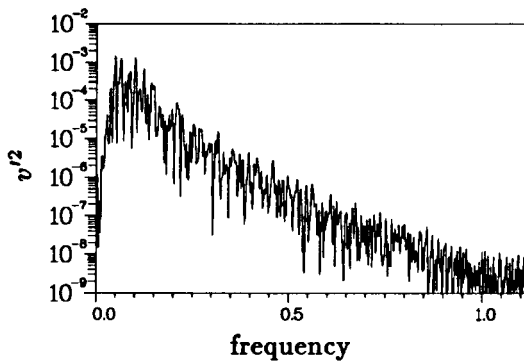### 4.2. Analysis of Discrete Sequences

Two goals of open-flow studies using nonlinear dynamics techniques are low-dimensional modeling and prediction. One way to do this is to extract from the data a discrete sequence of significant events, such as vortex passage periods T, vortex strengths or any other significant dynamic measure. From this sequence, first-return maps (T_n versus T_{n+1}) can be constructed which give information about what the next period will be based on the previous period. If these maps are highly ordered, a curve fit might give a useful predictive model. If the maps are less structured, it may still be possible to quantify how much information is "stored" by the flow system – about the future based on the past – by computing "stored information" (Shaw 1984). We constructed first-return maps from periods between zero-crossings of v and computed stored information:

$$\mathbf{I}(T_{n+1}|T_n) = \int P(T_n) \int P(T_{n+1}|T_n) \log(P(T_{n+1}|T_n)/P(T_n)) dT_{n+1} dT_n$$

where $\mathbf{I}(T_{n+1}|T_n)$ is the stored information, $P(T_n)$ is the probability density function (pdf) of T_n, and $P(T_{n+1}|T_n)$ is the pdf of T_{n+1} conditional on T_n. Unfortunately, to construct a convergent pdf estimate requires a large number of points, particularly when one wishes to construct conditional pdfs from some subset of the data set. As a result, we were unable to get useful results from our data, which had less than 200 structure passages (when we needed of the order of thousands). The pdfs and stored information were quite sensitive to number of bins used in the pdf estimate. The stored information fluctuated significantly as number of bins was changed. We were unable to establish reliably even an approximate value which could reveal trends in $\mathbf{I}(T_{n+1}|T_n)$ as location was changed.

(a)

(b)

FIGURE 3. Spectrum of v for case (i), $a = b = c = 0$; (a) $x = 140$, (b) $x = 230$.

5. Results and Discussion

Case (i): $(a = b = c = 0)$

Velocity spectra in the unforced case showed no sharp peaks: a broadband fundamental peak appeared at small x (figure 3a) and was replaced at larger x by a broadband subharmonic peak (figure 3b). Computation of the correlation integral revealed no scaling region. This is not unexpected; the instability is driven by ambient perturbations only, which are almost entirely boundary condition reflections at the outflow. For the computational domain chosen, the reflection was weak and aperiodic (Buell & Huerre 1988). Since the reflections are not periodic, the fluctuations passing the "probe" are necessarily not. Due to the lack of scaling, no parameters could be extracted to compute Lyapunov exponent.

Case (ii(a)): $(a = 0.01; b = c = 0)$

The fundamental was forced at $\omega = 0.18$. Traces of v velocity at four different x locations (figure 4) show how the flow is periodic at $x = 100$ and becomes more disordered with increasing x. At $x = 140$, the emergence of the subharmonic component can be seen in the alternating higher and lower peaks at some times. At $x = 170$ and 200, events can be seen with twice the period of the fundamental; this is the footprint of paired vortices. Spectra of v velocity (figures 5a-d) at the same
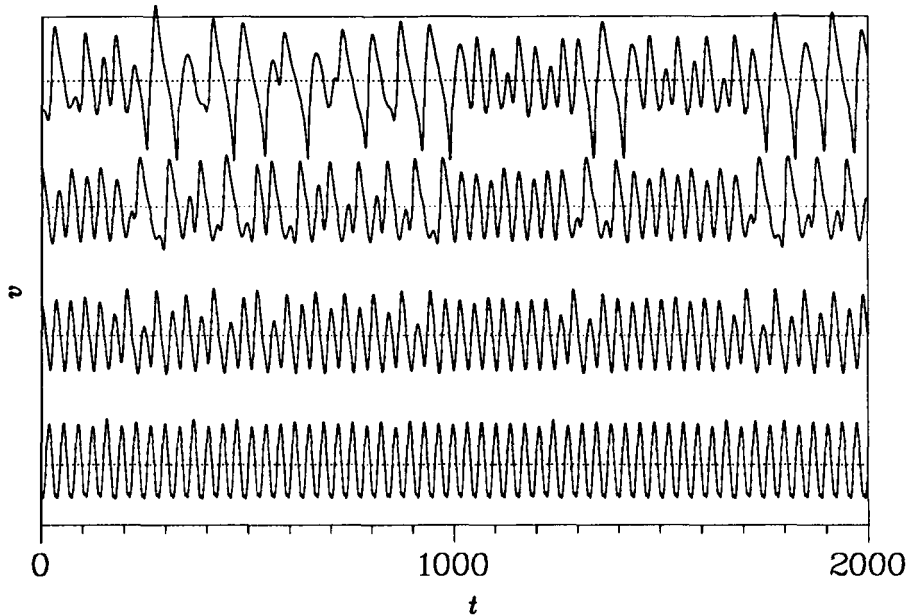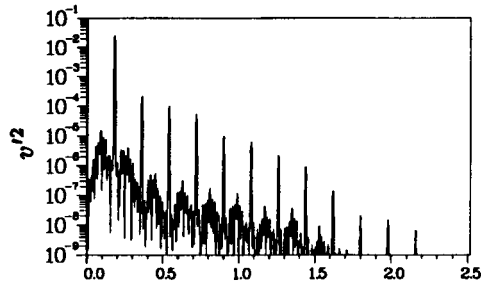
FIGURE 4. Time traces of v for case (ii(a)), $a = b = 0.01$, $c = 0$; from bottom to top, $x = 100, 140, 170, 200$.
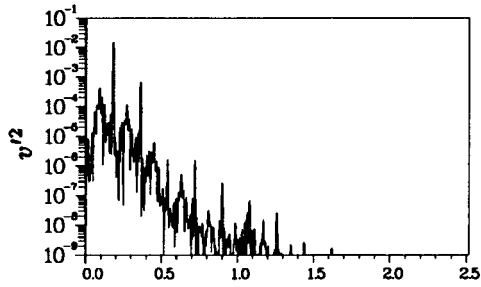
locations reveal sharp peaks at the fundamental frequency and its harmonics which slowly diminish with x. The peak of the subharmonic is not sharp, however; it forms a noisy narrowband peak at about $\omega = 0.09$. This peak is initially quite low: at $x = 100$ (figure 5a), the fundamental is almost 4 orders of magnitude higher; at $x = 140$ (figure 5b), the fundamental is 2 decades higher; at $x = 170$ (figure 5c), the peaks are only a decade apart; and at $x = 200$ (figure 5d), the noisy subharmonic clearly dominates the spectrum. At this point, the spectrum looks quite similar to the spectrum in the unforced case (figure 3b). This is not surprising, since the subharmonic was unforced in both cases.

In contrast with case (i), correlation integral calculations worked quite well in this case. Results for cases (ii(a)) and (ii(b)) are shown in figure 6. For case (ii(a)), correlation dimension was near 1 for $x < 100$ and increased monotonically to a value between 3 and 4 by $x = 170$. For locations $x > 170$, the correlation integral did not truly scale. An oscillation in the slope sometimes appears at high embedding dimensions which obscures any flat slope; in other cases the slope is flat but still rises a few percent with each higher embedding dimension. In all cases, at large x, the scaling region is quite small, extending over a factor of two or less in distance. This is quite likely due to a lack of long time series, as discussed above in Analysis Techniques. Time series of only 9000 points (188 orbits) were used. The values shown in figure 6 for $x > 170$ are estimates from the time series available; the true dimension is likely to be higher.
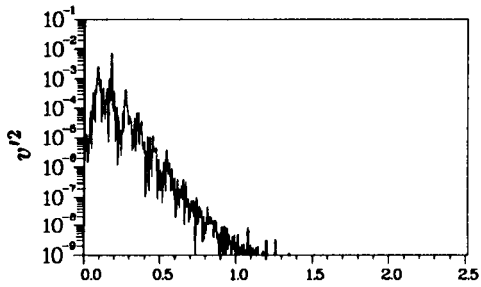
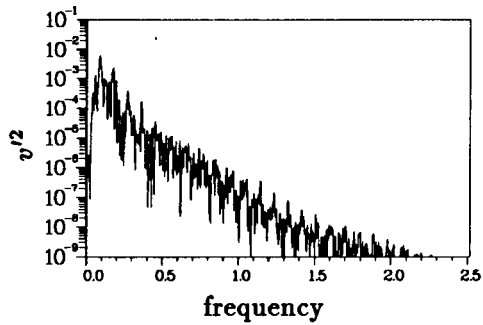Calculation of the largest Lyapunov exponent over the domain $100 \le x \le 200$ did

(a)

(b)

(c)

(d)

FIGURE 5. Spectra of v corresponding to figure 4; (a) $x = 100$, (b) $x = 140$, (c) $x = 170$, (d) $x = 200$.
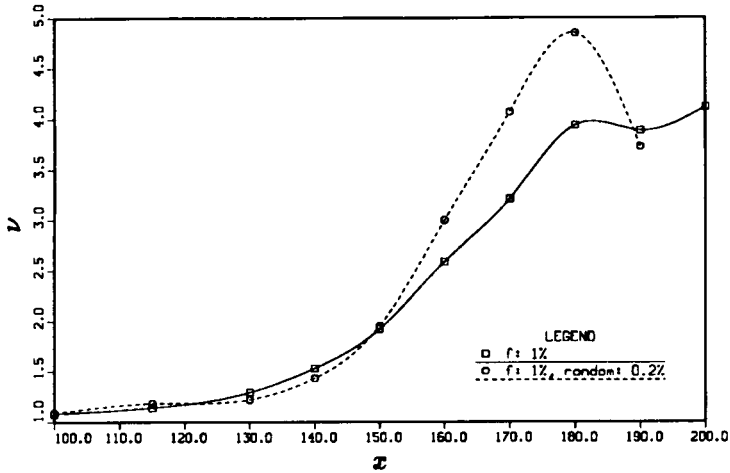
FIGURE 6. Correlation dimension as a function of location for cases (ii(a)) and (ii(b)).

not show an appreciable positive value at any location. Values ranged from -0.0083 bits/orbit (-0.00023 bits/time unit) to 0.072 bits/orbit (0.002 bits/time unit), showing a general, though not monotonic, increase with x. While the largest value found might indicate chaos, this possibility is not certain. These exponents can be interpreted as the average rate at which information is lost or gained about the initial condition of a phase space trajectory; a positive value represents a loss of information and therefore sensitive dependence on initial condition. The largest calculated value can be compared loosely with values reported by Wolf *et al.* (1985) for the Lorenz attractor (2.16 bits/time unit, 1.08 bits/orbit) and the Rossler attractor (0.13 bits/time unit, 0.78 bits/orbit) for typical parameter values.

Case (ii(b)): $(a = 0.01; \ b = 0; \ c = 0.01)$

Since the boundary condition reflection was difficult to quantify but was clearly not periodic, we imposed a random perturbation on the inlet in addition to the fundamental perturbation. This perturbation was designed to be of lower amplitude than the fundamental but higher than the background. At the first x station ($x = 0.7$), the fundamental amplitude of the v spectrum was 10^{-5}, while the white noise amplitude was 10^{-10} (figure 7). For the case with no random input, the background amplitude was less than 10^{-11}. Spectral development is quite similar to that of the case with no random forcing, as was that of dimension (figure 6) and Lyapunov exponent. The two dimensions begin to deviate after $x = 160$; exact values at larger x are unreliable, but the trend seems to indicate that the system under random forcing may have higher dimension. The drop in dimension for the randomly forced case at $x = 190$ is clearly not physical; it is most likely due to the lack of data records of adequate length.

Case (iii): $(a = 0.01; \ b = 0.01, \ b = 0.002, \ 0.0005; \ c = 0)$

This case yielded both expected and unusual results. Intuition suggests that the
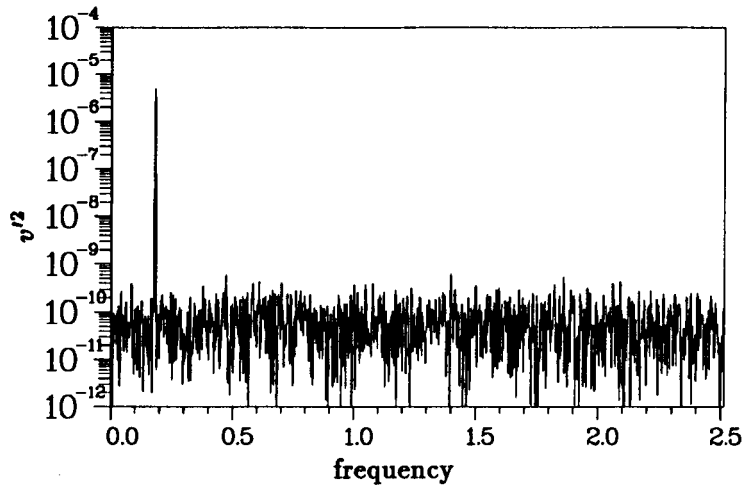
FIGURE 7. Spectrum of v at first x station for case (ii(b)), $a = 0.01$, $b = 0$, $c = 0.01$.
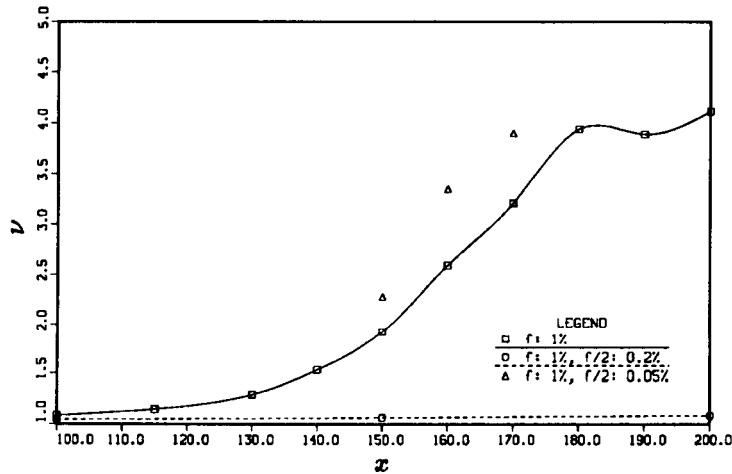

FIGURE 8. Correlation dimension as a function of location for cases (ii(a)) and (iii).

presence of sinusoidal fundamental and subharmonic should make the flow periodic for a larger streamwise distance. When the subharmonic amplitude was 1% and 0.2%, this was the case; in fact, the flow was periodic and dimension was 1 throughout the domain (figure 8). When the subharmonic was very low (0.05%), however, the flow was not periodic, and had higher dimension than with no subharmonic forcing at all. This is contrary to intuition, since we expect that even a low amplitude subharmonic would organize the flow more than no subharmonic at all. As a check, spectra with and without this forcing were compared, and they revealed that the noisy subharmonic had higher amplitude with the forcing. Further investigation showed that the forcing amplitude was of the order of reflection noise. We speculate

that superposition of subharmonic forcing with the boundary condition reflections creates higher subharmonic amplitude which is still noisy.

The results of cases (ii(a)) and (ii(b)) seem to indicate chaotic behavior. The growth of narrowband noise in the spectrum, exponential falloff of spectra at high frequencies for large x and the increase from unity of correlation dimension all point to the presence of low dimensional chaos in this system. By comparing the development in x of the spectrum with correlation dimension, one sees the connection between dimension and the growth of the subharmonic. The fundamental excitation has caused the flow to be periodic for small x, but the subharmonic does not grow from a pure sinusoid and its contribution to the dynamics is necessarily aperiodic. As the subharmonic grows, the flow becomes less organized; however, this disorganization appears to be low dimensional chaos.

The similarity between cases (ii(a)) and (ii(b)) is quite significant. The boundary condition reflection can not be entirely random; reflections will peak as large structures pass out of the computational window, yielding a broadband reflection centered at the subharmonic frequency, as there is only one pairing within the computational domain. The random forcing is white (figure 7). But the flow driven by weak internal reflections and the flow driven by white noise are similar: these perturbations are organized by the secondary instability into a low-dimensional chaotic flow rather than a random flow. However, this low-dimensional behavior is observed only in forced cases with periodic roll up; the unforced case showed no scaling at all. Why is this? Perhaps the answer lies with the subharmonic resonance phenomenon, which has been investigated both theoretically (Monkewitz 1988) and experimentally (Husain & Hussain 1986). Comparing spectra in cases (i) and (ii(a)), the bandwidth of the unforced flow (figure 3a) is significantly broader than that of the subharmonic component in the forced flow (*e.g.*, figure 5b). Because we have supplied a single fundamental frequency ω, it resonates most strongly with the frequency $\omega/2$. Other frequencies near $\omega/2$ will resonate because of detuning, but their amplitudes will be lower. However, if the fundamental is narrowband rather than a sharp peak, resonance will occur over a wider range of frequencies, giving a wider subharmonic bandwidth. Thus, the flow with no forcing has a wider spectral band in both the fundamental and subharmonic. This lack of organization must result in higher dimension, too high to be measured with the record length available. The linear falloff at high frequencies in case (i) and in cases (ii(a,b)) points to deterministic chaos in this flow (Sigeti & Horsthemke 1987), although we could not measure its dimension.

6. Concluding Remarks

A numerically generated, two-stream mixing layer has been studied as a function of position in an Eulerian frame for evidence of temporal chaos. The most interesting result was for cases in which a single, periodic perturbation was imposed at the inlet. With increasing x, narrowband peaks developed in the spectra, dimension increased from 1, and spectra at high frequencies fall exponentially, indicating that the flow had become chaotic.

The absence of a positive Lyapunov exponent is puzzling in light of other indicators of chaos. The recent work of Deissler and Kaneko (1987) shows, using the Ginzburg-Landau equation and coupled logistic maps, that convectively unstable systems which appear chaotic may nonetheless have zero Lyapunov exponent when measured in a stationary frame. However, positive Lyapunov exponents were measured in a frame moving with the disturbance. The mixing layer is a convectively unstable flow and may exhibit the same behavior. Additional study will be focused on this possibility.

The development of chaos in the singly forced case can be seen as the result of resonance between the periodic fundamental and its subharmonic. Since the ambient fluctuations are broadband, the subharmonic develops as a narrow band rather than a single frequency due to detuning. The layer shows qualitatively the same behavior when forced with fundamental alone as when forced with fundamental and random noise. This is quite interesting because the perturbation sources are quite different: in one case the source is reflections which are due to downstream flow conditions, whereas in the other case it is imposed random perturbations. More investigation is necessary to determine whether this similarity is superficial or there is some universality to the dynamics regardless of the extrinsic perturbation.

Laboratory experiments will serve as an important test of these results. Will the flow evolve similarly in the laboratory, or will the low-dimensional dynamics be overcome by three-dimensional phenomena? Three-dimensional mixing layers should behave quite differently. The onset of the spanwise secondary instability, the development of ribs, the possibility of vortex cut-and-connect and the breakdown of the mixing layer are important dynamic events which are not possible in two dimensions. In addition, 3-D spatially developing simulations and simulations of temporally developing flows will be quite important to study these phenomena as low-dimensional dynamical systems under carefully controlled conditions.

REFERENCES

BECHERT, D. 1985 *Z. Flugwiss. Weltraumforschung* **9**, 356.

BRANDSTATER, A. & SWINNEY, H.L. 1987 *Phys. Rev. A* **35**, 2207.

BUELL, J. & HUERRE, P. 1988, elsewhere in the volume.

CAIN, A. B., FERZIGER, J. H. & REYNOLDS, W. C. 1984 *J. Comp. Phys.* **56**, 272-286.

DEISSLER, R.J. & KANEKO, K. 1987 *Physics Letters A* **119**, 397.

FRASER, A.M. & SWINNEY, H.L. 1986 *Phys. Rev. A* **33**, 1134.

GRASSBERGER, P. & PROCACCIA, I. 1983 *Phys. Rev. Lett.* **50** , 346; 1983 *Physica* **9D**, 189.

HUSAIN, H.S. & HUSSAIN, A.K.M.F. 1986 *Bull. Am. Phys. Soc.* **31**, 1696.

HUSAIN, H.S. & HUSSAIN, F. 1988 Subharmonic Resonance in a Shear Layer, presented at the 2nd European Turbulence Conference, Berlin.

KIM, J. & MOIN, P. 1985 *J. Comp. Phys.* **59**, 308-323.

MONKEWITZ, P. A. 1988 *J. Fluid Mech.* **188**, 223.

SAULIERE & HUERRE, P. 1988, private communication from Patrick Huerre.

SHAW, R. 1984 *The Dripping Faucet as a Model Chaotic System.* Aerial Press.

SIGETI, D. & HORSTHEMKE, W. 1987 *Phys. Rev. A* **35**, 276.

TAKENS, F. 1980 in: Proc. Warwick Symp., D. Rand and B. S. Young, eds, *Lecture Notes in Math.* **898** (Springer, Berlin, 1981).

WOLF, A., SWIFT, J., SWINNEY, H.L & VASTANO, J.A. 1985 *Physica* **16D**, 285.

WRAY, A. A. 1988 submitted to *J. Comp. Phys.*